



BNL-94970-2011-CP

***Rogue Mode Shielding in NSLS-II Multipole
Vacuum Chambers***

*A. Blednykh[#], B. Bacha, A. Borrelli, M. Ferreira, H.-C. Hseuh, B. Kosciuk, S.
Krinsky, O. Singh, K. Vetter*

*Presented at the 2011 Particle Accelerator Conference (PAC'11)
New York, NY
March 28-April 1, 2011*

March 2011

**Photon Sciences Directorate
Brookhaven National Laboratory**

**U.S. Department of Energy
DOE - Office of Science**

Notice: This manuscript has been authored by employees of Brookhaven Science Associates, LLC under Contract No. DE-AC02-98CH10886 with the U.S. Department of Energy. The publisher by accepting the manuscript for publication acknowledges that the United States Government retains a non-exclusive, paid-up, irrevocable, world-wide license to publish or reproduce the published form of this manuscript, or allow others to do so, for United States Government purposes.

This preprint is intended for publication in a journal or proceedings. Since changes may be made before publication, it may not be cited or reproduced without the author's permission.

DISCLAIMER

This report was prepared as an account of work sponsored by an agency of the United States Government. Neither the United States Government nor any agency thereof, nor any of their employees, nor any of their contractors, subcontractors, or their employees, makes any warranty, express or implied, or assumes any legal liability or responsibility for the accuracy, completeness, or any third party's use or the results of such use of any information, apparatus, product, or process disclosed, or represents that its use would not infringe privately owned rights. Reference herein to any specific commercial product, process, or service by trade name, trademark, manufacturer, or otherwise, does not necessarily constitute or imply its endorsement, recommendation, or favoring by the United States Government or any agency thereof or its contractors or subcontractors. The views and opinions of authors expressed herein do not necessarily state or reflect those of the United States Government or any agency thereof.

ROGUE MODE SHIELDING IN NSLS-II MULTIPOLE VACUUM CHAMBERS*

A. Blednykh[#], B. Bacha, A. Borrelli, M. Ferreira, H.-C. Hseuh, B. Kosciuk, S. Krinsky, O. Singh, K. Vetter, BNL, NSLS-II, NY 11973-5000, U.S.A.

Abstract

Modes with transverse electric field (TE-modes) in the NSLS-II multipole vacuum chamber can be generated at frequencies above 450MHz due to its geometric dimensions. Since the NSLS-II BPM system monitors signals within 10 MHz band at RF frequency of 500 MHz, frequencies of higher-order modes (HOM) can be generated within the transmission band of the band pass filter. In order to avoid systematic errors in the NSLS-II BPM system, we introduced frequency shift of HOMs by using RF metal shielding located in the antechamber slot.

INTRODUCTION

A new 3GeV NSLS-II storage ring is under construction at Brookhaven National Laboratory. The ring has a 30 cell double-bend achromatic (DBA) lattice [1]. Six beam position monitors (button type) per cell are going to be located on multipole vacuum chambers to control electron beam trajectory. Each vacuum chamber in each cell is numerated in according to girder location. Five types of multipole vacuum chambers are going to be used in the NSLS-II storage ring [1]. They have the same cross-section profile and differ mostly in length. Multipole vacuum chambers S2, S4 and S6 are shown in Figure 1 with location of BPM Buttons.

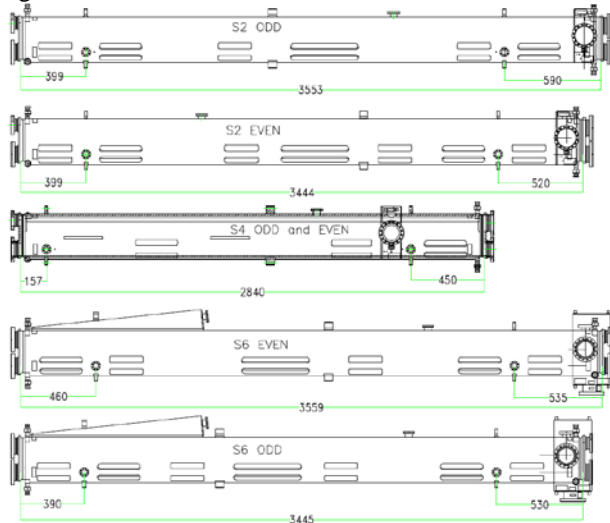


Figure 1: Types of NSLS-II multipole vacuum chambers.

The NSLS-II multipole vacuum chamber profile is shown in Figure 2. The full horizontal and vertical aperture of the beam channel is 76mm x 25mm

respectively. The antechamber slot with a gap of 10mm is extended up to a trapezoidal area with a vertical aperture of 44mm. The NSLS-II cross-section profile has a complex geometry and looks similar to APS chamber design, except a difference in geometric dimensions. There is a concern that existence of rogue modes observed in vacuum chambers with antechamber slot [2] can affect precision of the NSLS-II BPM diagnostic system. As in APS, the NSLS-II BPM buttons are located on top and bottom of multipole vacuum chambers, which have an antechamber slot (Fig. 2). Rogue modes, which are classified as modes with Transverse Electric field (H-mode) in a ridged waveguide, can couple to the BPM buttons at frequencies near to the RF. It can produce a noise in BPM system and difficulties in monitoring of beam position in the ring.

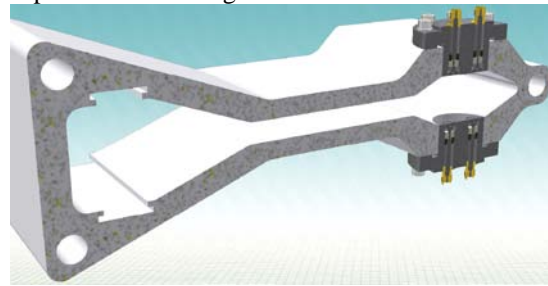


Figure 2: NSLS-II multipole vacuum chamber profile.

Since the NSLS-II multipole vacuum chamber profile has a complex geometry, the cutoff wavelength has been simulated numerically using the GdfidL code [3]

$$\lambda_c = 0.695m.$$

Since the cutoff wave length is known a set of resonance modes can be generated in a chamber at frequencies

$$f_{mnp}^H = \frac{c}{2\pi} \sqrt{\left(\frac{2\pi}{\lambda_c}\right)^2 + \left(\frac{p\pi}{L}\right)^2},$$

where c is the velocity of light, λ_c is the cutoff wavelength, $p=1,2,\dots,k$ and L is the chamber length. Based on Maxwell's equations the first lowest mode like in a ridged cavity depends on the structure length (H_{101} -mode). Index p cannot be equal zero ($p \neq 0$). For a length of $L=3553mm$ (length of the S2-chamber), the first resonant frequency is $f_{101}^H = 434MHz$. It agrees well with the frequency of the dominant mode obtained due to numerical simulations and microwave measurements (Table 1). Frequencies of the first six H_{mnp} -modes are shown in Table 1. The frequency of H_{106} -mode is almost equal to the RF frequency. In order to avoid interference

*Work supported by DOE contract No: DE-AC02-98CH10886

[#]blednykh@bnl.gov

of H-modes (TE-modes) with the BPM signal, the RF shielding is required.

Table 1: Frequency comparison of the H_{10p} -modes for the multipole vacuum chamber with a length of 3553mm

Mode	Measurements f, MHz	GdfidL f, MHz	Equation f, MHz																
H_{101}	430	434	434																
H_{102}	436	440	440																
H_{103}	446	450	450 </tr <tr> <td>H_{104}</td> <td>458</td> <td>463</td> <td>464</td> </tr> <tr> <td>H_{105}</td> <td>478</td> <td>480</td> <td>481</td> </tr> <tr> <td>H_{106}</td> <td>496</td> <td>500</td> <td>501</td> </tr> <tr> <td>H_{107}</td> <td>518</td> <td>523</td> <td>523</td> </tr>	H_{104}	458	463	464	H_{105}	478	480	481	H_{106}	496	500	501	H_{107}	518	523	523
H_{104}	458	463	464																
H_{105}	478	480	481																
H_{106}	496	500	501																
H_{107}	518	523	523																

ROGUE MODES SHIELDING REQUIREMENTS

The NSLS-II RF BPM electronics [4] employ a sub-sampling architecture whereby the fundamental 500MHz RF signal is under-sampled at ~ 117 MHz utilizing 16b ADC's. The short pulses produced by the button pickups are passed through the high-band of a diplexer located 1m from the pickup. The resultant high-band diplexer output corresponds to the 5th-order Bessel impulse response centered at 500MHz. The low-band of the diplexer centered at 470MHz is used to inject a calibration tone.

The BPM spectral region of concern illustrating the desired rogue mode attenuation profile derived from an RF BPM signal processing perspective is shown below in Fig. 3. The horizontal axis is frequency in MHz, the left vertical axis is power relative to milliwatt (dBm), and the right vertical axis is power relative to the BPM pickup port seen by the RF BPM (i.e. dB_{pu}).

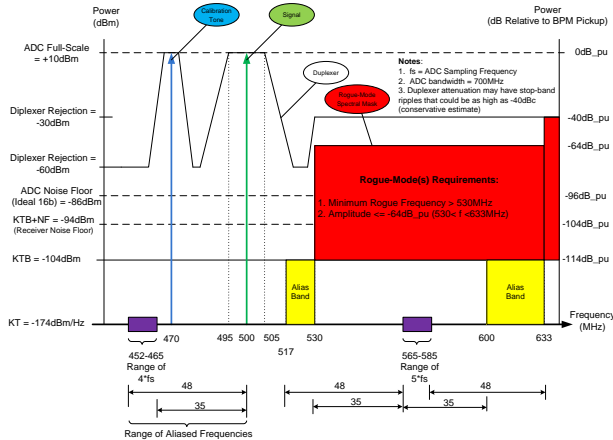


Figure 3: Rogue-Mode RF BPM Requirements.

The horizontal axis also illustrates two harmonic sampling regions (452-465, and 565-585MHz). These regions correspond to the 4th and 5th harmonics of the sampling clock of the ADC. The baseband digital signal processing operates on an intermediate frequency resulting from aliasing of the 500MHz signal with the 4th sampling harmonic. The fundamental sampling frequency of the ADC can range from 113MHz to 117MHz. As a result of bandpass sampling two alias regions of concern relative to the 5th sampling harmonic exist. These two regions are illustrated in yellow (517MHz – 530MHz, and 600MHz – 633MHz).

The desired rogue mode spectral mask has been defined in red considering the aliasing regions, finite attenuation of the diplexer, and the system noise floor. For the first requirement it would be desirable that no rogue modes exist below 530MHz. Rogue mode energy below 530MHz could potentially result in inter-modulation distortion (IMD) products that fall in-band. These in-band IMD products could either bias the position measurement, or add a time-varying component to the position measurement. The 2nd requirement would be for the BPM Pickup signal power to be less than -64dB_{pu} for the region between 530MHz to 633MHz. For a mode at -64dB_{pu} the 40dB of attenuation introduced by the diplexer high-band will push the mode down to the noise floor of -104dB_{pu} (-94dBm at receiver input). The rogue mode power above 633MHz is less of a concern as a result of the ADC response roll off starting at 700MHz combined with an anti-aliasing low pass filter with a cutoff frequency of 550MHz.

BASIC CONCEPT OF ROGUE MODE SHIELDING

All dimensions of the NSLS-II multipole vacuum chamber are already fixed and cannot be changed. The RF frequency is chosen to be 499.68MHz. Due to user requirements, we cannot keep a fixed fill pattern with bunch frequency less than 400MHz. To protect the NSLS-II BPM Buttons from the electric field of H_{mnp} -modes the RF shielding will be installed in each multipole vacuum chamber.

One way to avoid signal interference with frequencies of rogue modes is a wideband frequency shift due to insertion of RF metal shielding into the chamber. Since the cutoff frequency f_c of the H_{10} -mode depends on geometric parameters such as a , a' , b and b' the width of the chamber can be reduced by introducing the RF shielding at a distance D as is shown in Fig. 4. It gives an opportunity to shift frequencies of H-modes above required frequency of 530 MHz.

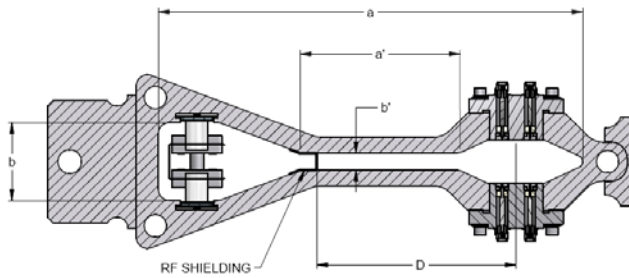


Figure 4: NSLS-II multipole vacuum chamber profile.

Vacuum requirements dictate that RF shielding should not significantly affect the performance of the getter strips located in the antechamber. A simple RF shielding design was chosen with a cross section shaped such that it could be inserted into the aft section of the 10mm extraction slot adjacent to the anti-chamber (Fig. 5). This is an ideal location in part because in five out of six BPM locations, ray tracings revealed no radiation here that could damage the shield. Beryllium copper (BeCu) was chosen for its high elastic modulus, giving the shield adequate spring force to retain it in the extraction slot. To satisfy the pumping requirement, it was necessary to perforate the face of the shield with roughly 50 percent transparency. This resulted in an array of 6.6mm square apertures spaced on 7.5mm intervals, small enough so the fields could not penetrate but large enough for adequate pumping. Notching the wings of the shield every 25mm allowed it to be produced using traditional progressive tool stamping technology which in turn allowed the shields to be produced in a continuous length then cut to the size needed for each chamber.

Installation is achieved by first positioning the shield inside the vacuum chamber against the back of the extraction slot. An insertion tool which is guided by the NEG slots is then pulled down the length of the chamber, seating the shield to the appropriate depth.



Figure 5: Flexible BeCu RF shielding with 50% of opening space inside of the multipole vacuum chamber. The thickness of the RF shielding is 0.25mm.

MICROWAVE MODE MEASUREMENTS IN CHAMBERS WITH RF SHIELDING

Three types of the multipole vacuum chamber have been measured; S2, S4 and S6 chambers with the length of 3553mm, 2840mm and 3445mm respectively. The S21-parameter has been measured through loop antennas installed on one side of the chamber and BPM buttons located on both sides of the chamber. Loop antennas can generate the whole frequency spectrum of H_{10p} -modes, whereas the BPM buttons can miss some of the mode, which have minimum electric field at the point of the BPM button location.

S4-Vacuum Chamber ($L=2840mm$)

S4 vacuum chamber has been loaded with flexible BeCu RF shielding at a distance $D=114mm$ from the beam pipe center. Two separate RF shields of 2.2m and 460mm length are required in order to provide shielding before and after the stick absorber (Fig. 1). Two loop antennas are mounted on a side of the vacuum chamber to generate fields of H_{10p} -modes. Transmission coefficients (S21-parameter) using two loop antennas, from button to button and from loop to button have been measured for frequency cross checking.

Figs. 6 and 7 present measured results of the transmission coefficients in S4 chamber. Since the stick absorber splits the chamber into two sections with different lengths we measured S21-parameter in each of the sections. In the long-length section the first resonant peak of H_{101} -mode is generated at frequency 923MHz (Fig. 6). In the short-length section the first lowest frequency is 929MHz (Fig. 7). The proposed shield works properly, effectively shifting the frequencies sufficiently higher than required.

Since S4 chamber has been extruded with a small difference in gap along longitudinal direction we had some difficulties to install RF shielding properly, using a brand new installation tool designed by B. Kosciuk. The gap is a bit smaller in the middle of the chamber than required. The RF shielding was installed manually and it can have some wave-form along the chamber. In this case first several peaks can correspond to H_{101} -mode at first few frequencies. In order to be sure, we measured the electric field distribution along the chamber at frequency 978MHz (Fig. 8, bead-pull measurements) using a thin metal disk. The horizontal axis in Fig. 8 corresponds to a chamber length of $L=2840mm$. As can be seen the electric field occurs at the beginning of the structure, on the length equivalent to one-eighth of the structure.

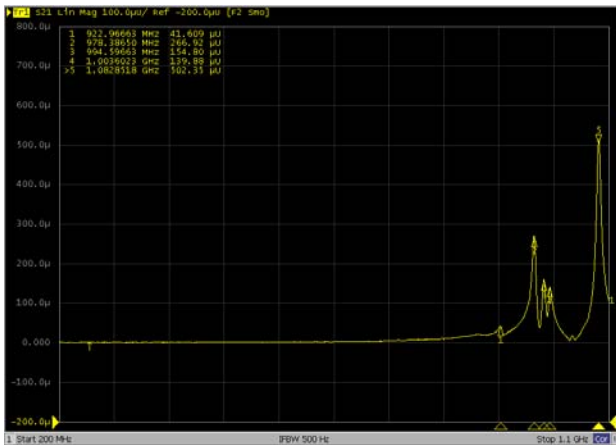


Figure 6: Measured S21-parameter in the long-length section of the S4 multipole vacuum chamber with RF shielding inside (linear scale). Loop to button.

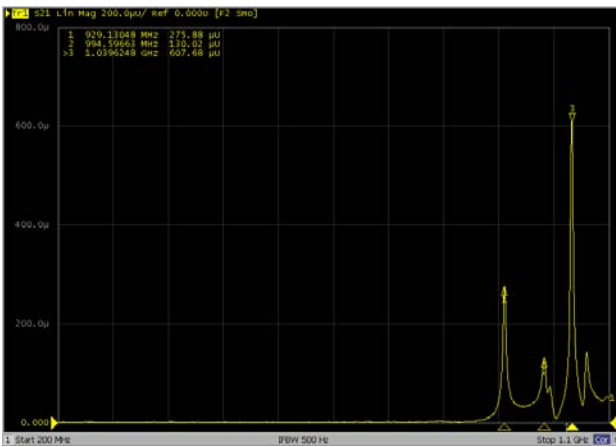


Figure 7: Measured S21-parameter in the short-length section of the S4 multipole vacuum chamber with RF shielding inside (linear scale). Loop to button.



Figure 8: Electric field distribution $|E_y|^2$ along the S4 chamber at frequency 978MHz in long-length section. Vertical field measured in the middle of the chamber.

S2-Vacuum Chamber ($L=3553mm$)

S2 odd chamber has been measured in the same manner as S4 chamber. Since the stick absorber is located close to end of the chamber, only one RF shield with a length of $\sim 3.5m$ has been loaded. In this case we applied an installation tool and based on measurement results no unexpected frequencies were found as in a case with S4 chamber. The lowest frequency measured in the chamber with RF shielding is 939MHz (Fig. 9). Measured electric field distribution at frequencies 939MHz and 948MHz is shown in Figs. 10a and 10b respectively.

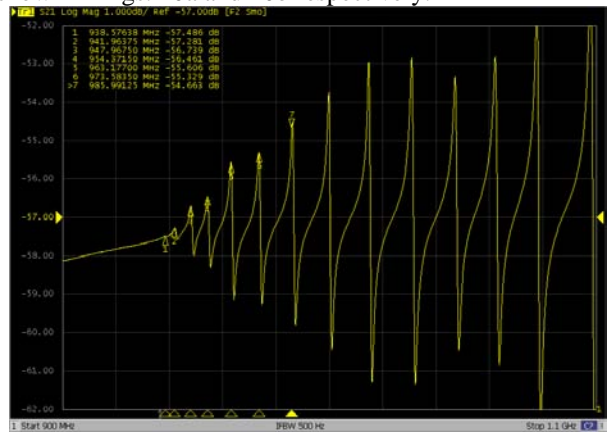


Figure 9: Measured S21-parameter in the S2 multipole vacuum chamber with RF shielding inside (logarithmic scale). Input and output signals are taken from loop antennas located on one side of the chamber.

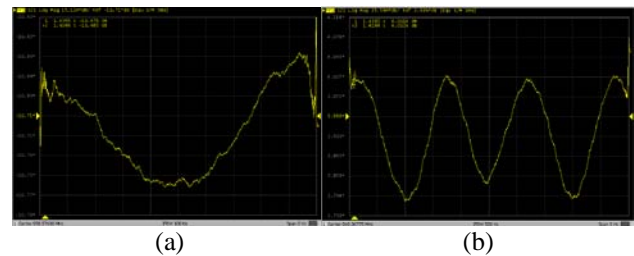


Figure 10: Measured electric field distribution $|E_y|^2$ along the S2 chamber at frequencies 939MHz (a) and 948MHz (b). Frequencies correspond to H_{101} -mode and H_{103} -mode respectively.

In Table 2 we compare measured frequencies versus numerically simulated. These results show that there is a slight difference between frequencies. It can be explained due to strong frequency dependence on D parameter. A bit larger/smaller pressure by installation can move RF shielding that can bring frequencies higher/lower.

The RF shielding was installed properly. Measured and simulated frequencies correspond to a different H_{10p} -mode. In Fig. 11 we plot electric field distribution simulated for the first few values of p ($p=1, 2$ and 3). The

red line is the field distribution $|E_y(L)|$ at frequency $f=954\text{MHz}$. It corresponds to H_{101} -mode. The blue dashed line is $|E_y(L)|$ at frequency $f=957\text{MHz}$. It corresponds to H_{102} -mode. The vertical field component E_y varies in the longitudinal direction depends on p -value.

Table 2: Frequencies of H_{10p} -modes in 3553m multipole vacuum chamber with the RF shielding inside

Mode	Measurements f, MHz	GdfidL f, MHz
H_{101}	939	954
H_{102}	942	957
H_{103}	948	962
H_{104}	954	968

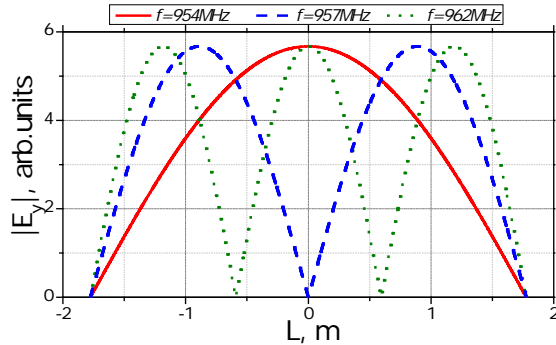


Figure 11: Numerically simulated electric field distribution inside the S2 chamber with RF shielding for first three values of p ($p=1, 2$ and 3). We show the results of $|E_y|$ as a function of chamber length L simulated in the middle of the chamber.

S6-Vacuum Chamber ($L=3445\text{mm}$)

The RF shielding length inside the S6 chamber has to stay clear of synchrotron radiation (red shaded color in Fig. 13) from downstream magnets. The emission angle in the horizontal direction at downstream of each S6 chamber is pretty large. The RF shielding has to be loaded at a distance of $\sim 2\text{m}$ away from the right side of the chamber (keeping the same horizontal distance of $D=114\text{mm}$) to avoid its heating and damage due to synchrotron radiation. The total inner length of the S6 even and odd chambers are 3559mm and 3445mm , respectively. It makes it hard to protect each downstream BPM Button in each S6 chamber with $\sim 2\text{m}$ of unshielded space.

We are considering two possibilities. First, the length of the RF shielding can be optimized so that 500MHz frequency can be centered between two neighboring

frequencies of H_{10p} -modes, which are generated in the empty space.

Measurements of the transmission coefficient using the downstream BPM buttons show that with a length of 2.1m unshielded space two neighboring peaks are seen at frequencies of 483MHz and 521MHz (Marker 3 and Marker 5 in Fig. 12). Marker 4 set up manually at frequency 500MHz . Perhaps tens of MHz criterion will be sufficient.

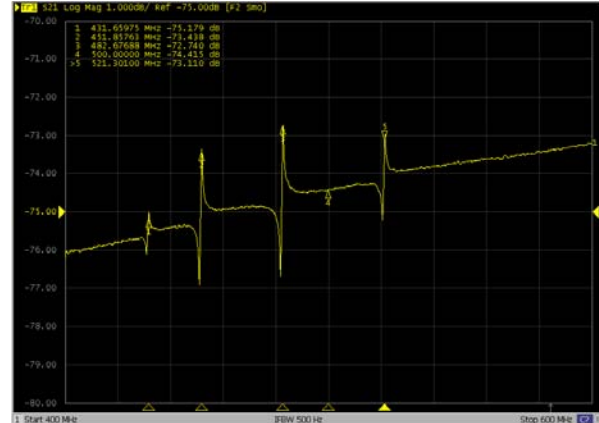


Figure 12: Measured S21-parameter in the S6 even multipole vacuum chamber with RF shielding inside (logarithmic scale). Location of the RF shielding is shown in Fig. 13. Input and output signals are taken from the downstream BPM button.

Second, if $\pm 15\text{MHz}$ frequency shift from 500MHz is not sufficient, then there is a risk to lose one BPM in each S6 chamber. To compensate it, ID BPM or high stability BPM are going to be located right after each S6 chamber in each straight section.

Measurements through the upstream BPM button (shielded area) show that the lowest frequency can be generated at $\sim 830\text{MHz}$. Electromagnetic fields generated in unshielded space (Fig. 12) at frequencies 432MHz , 451MHz and etc. are not seen by the upstream BPM button.

CONCLUSION

We demonstrated numerical modeling and experimental studies of the spurious TE modes in the NSLS-II vacuum chambers with antechamber slot. Calculated frequencies of TE-modes in considered chambers with and without RF shielding were verified experimentally. Flexible BeCu RF shielding inside each chamber at proper location shifts frequencies of H_{10p} -modes above $\sim 900\text{MHz}$, except chambers S6 odd and even. These chambers need special attention because of synchrotron radiation from downstream magnets.

S6 odd multipole vacuum chamber needs to be measured and the RF shielding length has to be optimized.

RF shielding looks adequate for baseline design. Fifty percent of open space provides adequate pumping speed.

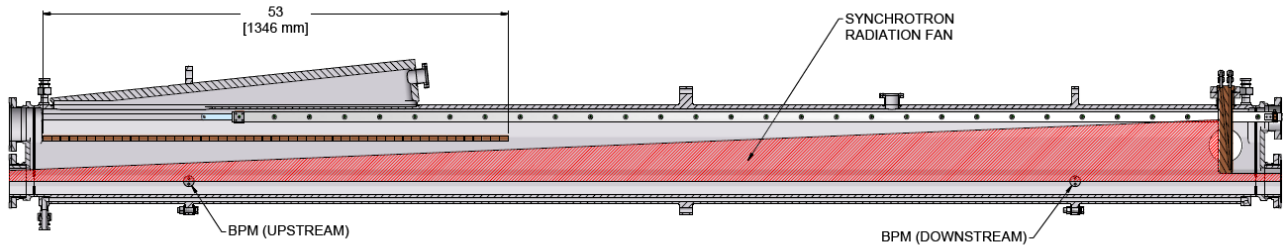


Figure 13: S6 even multipole vacuum chamber with RF shielding inside. The red shaded region represents the synchrotron radiation fan. Flexible BeCu RF shielding is 1346mm long.

ACKNOWLEDGEMENT

We thank Glenn Decker (APS/ANL), John Hoyt (APS/ANL), Bob Lill (APS/ANL), Mike Blaskiewicz (CAD/BNL) and Sushil Sharma (NSLS-II/BNL) for participating in review of the RF shielding for the rogue modes in the NSLS-II vacuum chamber and for their expertise and contribution to the design process.

REFERENCES

- [1] NSLS-II Preliminary Design Report, 2008; <http://www.bnl.gov/nsls2/project/PDR/>
- [2] Y. Kang, G. Decker and J. Song, "Damping spurious harmonic resonances in the APS storage ring beam chamber," EPAC'96, Sitges, June 1996, p. 7984.
- [3] W. Bruns, GdfidL code; <http://www.gdfidl.de>
- [4] K.Vetter et al., "NSLS-II RF Beam Position Monitor", BIW10, Sante Fe, NM. Current proceedings.